CHAPTER 3

In cellulo investigations of transcription factor p53 during genomic oxidative stress

Genomic sequencing conducted by the Millard and Muriel Jacobs Genetics and Genomics Laboratory at the California Institute of Technology.

INTRODUCTION

Gene regulation is the primary, and most well studied, role of transcription factor p53 in the human cell. It is generally accepted that gene regulation is initiated in a p53-dependent manner through the specific binding to defined response elements in the upstream regulatory region of certain genes. However, it currently remains unknown how p53 binding precisely results in the activation of certain genes, while simultaneously acting as a repressor for others.[1,2] Not only does p53 regulate protein production of well over a hundred confirmed genes, an emerging body of data also indicates that it may also play a pivotal role in genome-wide and cell type-specific changes in microRNA expression.[3]

Since we determined that p53 dissociates from DNA via oxidative DNA-mediated CT and that this dissociation is dependent upon guanine bases within the response element *in vitro*, we asked whether this response correlates to p53 activity during genomic stress *in cellulo*.[4] Preliminary research was conducted to determine whether this response correlated *in cellulo* by monitoring the levels of gene transcripts under p53 regulatory control via reverse transcription (RT) quantitative polymerase chain reaction (qPCR). For these experiments HCT116N cells were used since they contain a wild-type p53; genomic oxidative stress was induced through treatment with $Rh(phi)_2(bpy)^{3+}$ and subsequent irradiation.[5] During these experiments, three p53-regulated gene products were monitored which had formerly been characterized *in vitro* by EMSA: Caspase1A (CASP), S100A2 (S100A), and ornithine decarboxylase (ODC).[6]

Caspase1A is a cysteine-dependent aspartate-directed protease that plays essential roles in apoptosis, necrosis, and inflammation.[7] The binding of p53 to this response

element promotes the production of caspase. The response element of Caspase1A is very similar to the synthetic AAA sequence, with an adenine triplet within the purine region and no guanine doublets or triplets in either of the complementary strands.[4,7] Through EMSA analysis, it was determined that p53 does not readily oxidatively dissociate from this response element, with a maximum of 6.4% dissociation upon 30 minutes of irradiation, as shown in Figure 3.1.[4]

Conversely, the S100A2 protein is intimately involved in cell cycle progression, cellular differentiation, and may function as a tumor suppressor.[8,9] When p53 is bound to this guanine-rich response element, production of the S100A2 protein is promoted. The S100A2 response element is very similar to the synthetic GGG sequence, containing two guanine triplets within the purine regions.[4] Through EMSA analysis it was observed that p53 does oxidatively dissociate from the response element, with a maximum of 14% dissociation upon 30 minutes of irradiation, as depicted in Figure 3.1.

Ornithine Decarboxylase (ODC) is the rate-limiting enzyme in the decarboxylation of ornithine, a product of the urea cycle, to form putrescine.[10,11] In healthy cells, putrescine is synthesized in small quantities since it is a necessary polyamine that acts as a growth factor for cell division; however, high levels of putrescine are cytotoxic. When p53 is bound to the ODC response element the production of ornithine decarboxylase is repressed. This response element is similar to the GGG/GGG synthetic sequence, containing guanine doublets and triplets in both complementary strands of the response element. We experimentally observed in EMSA analysis that p53 oxidatively dissociates from this sequence, around 14.2% but with a drastically wide range of error, as seen in Figure 3.1.

FIGURE 3.1 — EMSA analysis (above) and corresponding preliminary RT-qPCR (below) of $Rh(phi)_2(bpy)^{3+}$-treated HCT116N cells to determine changes in p53 gene regulation. RT-qPCR Samples were normalized to the untreated control and the data represents the fold change in mRNA levels with respect to the control. The p53 response element sequences are located below the plots.[4,5]

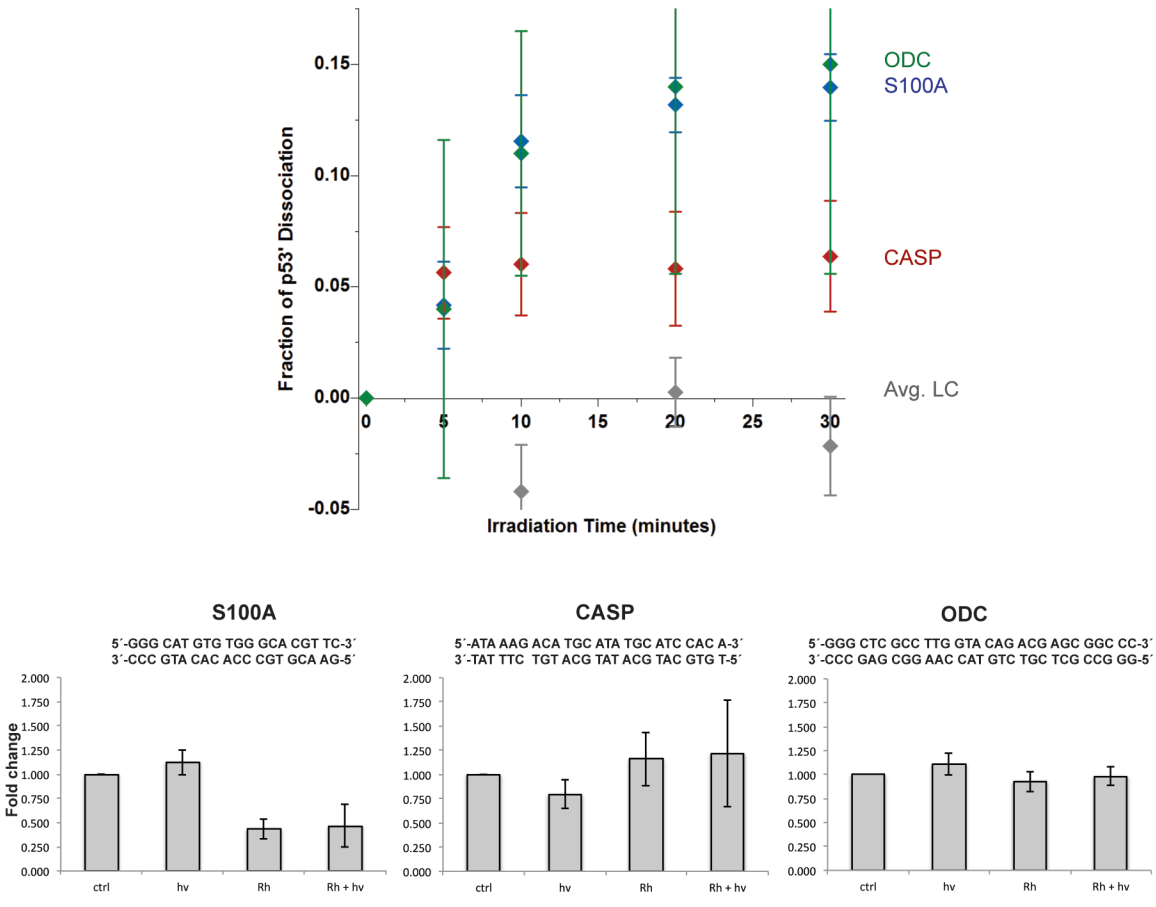

To examine the parallels of these EMSA data *in cellulo*, preliminary RT-qPCR trials were conducted.[5] The RT-qPCR results for S100A, as depicted in Figure 3.1, display a slight increase in gene product with irradiation without Rh treatment (-Rh). However, the Rh treated (+Rh) samples both showed a marked attenuation in the S100A gene product, even without irradiation. This indicates that the addition of Rh may be interfering with other cellular processes, leading to an overall decrease in S100A production solely due to the presence of Rh intracellularly. Since we did observe oxidative dissociation from the S100A response element *in vitro,* and p53 acts as a promoter for this gene, a correlating decrease in S100A gene product was anticipated for the +Rh-irradiated sample. The +Rh-irradiated samples for S100A showed attenuation within error of the +Rh-unirradiated samples, indicating no significant change in gene regulation occurred by inducing oxidative DNA CT.

In the case of Caspase1A, since p53 does not readily dissociate from this sequence *in vitro,* we would anticipate a continued or upregulated production of this gene transcript under conditions of oxidative genomic stress. The RT-qPCR results indicated a slight decrease in mRNA levels in the -Rh-irradiated samples, and a slight increase in the +Rh-unirradiated samples. When oxidative DNA CT was induced in the +Rh-irradiated samples, we observed a slight increase over the +Rh-unirradiated sample, and a much larger margin of variability.

With respect to ODC, which p53 dissociated from *in vitro* and functions as a repressor intracellularly, we would anticipate the dissociation of p53 to lead to an increase of ODC production. However, all experimental conditions were within error of

one another. Thus, despite thorough experimentation, no conclusions could be drawn by RT-qPCR.

To more directly probe the changes in p53 binding in response to oxidative DNA CT *in cellulo*, we decided to investigate the changes of p53 binding more directly through chromatin immunoprecipitation (ChIP). This technique allows the isolation of genomic fragments in direct contact with p53, which are then quantified through qPCR. This technique allows us to determine the occupancy of p53 at specific genomic locations in HCT116N cells under varied conditions. To gain more insight into p53 binding *in cellulo* during oxidative genomic stress, the isolated ChIP chromatin fragments were sequenced (ChIP-Seq) and aligned to the human genome. Lastly, from this ChIP-Seq data we were able to return to our former sets of ChIP DNA and explore other genomic sites showing p53 occupancy by qPCR.

MATERIALS AND METHODS

HCT116N cell growth. HCT116N cells were cultured at 37 °C with 5% carbon dioxide in RPMI medium 1640 supplemented with 10% FBS, 2 mM L-glutamine, 0.1 mM nonessential amino acids, 1 mM sodium pyruvate, 100 units/mL penicillin, 100 μg/mL streptomycin, and 400 μg/mL Geneticin. Two 75 cm^2 flasks of HCT116N cells were grown in complete HCT116 media, seeded from 1 million cells from cryostorage. The cells were grown until nearly confluent, harvested by trypsonization, combined, and split among four 500 cm^2 plates with 100 ml of complete media in each. Growth was allowed to continue for about two more days, until a confluence of about 30% was reached.

Rhodium photooxidant. [$Rh(phi)_2bpy]^{3+}$ (phi= 9,10-phenanthrenequinone diimine) was used in the following experiments to induce oxidative genomic stress within the HCT116N cells. The complex was made as previously described and synthesized by Ariel Furst for use in the ChIP experiments.[12]

$[Rh(phi)_2bpy]^{3+}$ treatment of HCT116N cells. Dry $Rh(phi)_2bpyCl_3$ was solvated in PBS buffer, sonicated to ensure a homogenous solution, and the concentration determined through UV-Visible spectroscopy (ε_{365} = 26300 nm). The HCT116N cells in a 500 cm^2 plate at 30% confluence were then dosed with 10 μM $[Rh(phi)_2bpy]^{3+}$ (+Rh) and 100 μl of DMSO in a total volume of 100 ml. The plates that were not treated with $[Rh(phi)_2bpy]^{3+}$ (-Rh) were treated with the same amount of PBS and DMSO as the +Rh samples. The cells were allowed to incubate at 37 °C for 16 h to internalize the complex.

Nutlin-3 treatment of HCT116N cells. Nutlin-3 was used to promote the upregulation of p53 through inhibiting MDM2 interaction. Following incubation with +Rh or -Rh, all four 500 cm^2 plates were washed twice with PBS, dosed with 50 mL 10 μM Nutlin-3 (Cayman Chemicals) in media, and allowed to incubate for 3 h at 37 °C. An example western blot depicting p53 upregulation is located in Appendix Figure 3.1. Treatment of the plates was staggered so that the +Rh treated samples were dosed with Nutlin-3 an hour prior to the -Rh samples. After 3 h of incubation in 10 μM Nutlin-3, the cells were washed twice with PBS and switched to 100 ml of 2.5 μM Nutlin-3 in PBS.

Irradiation. Samples were then irradiated for 45 minutes using a Solar Simulator (Oriel Instruments) equipped with a 1000W Hg/Xe lamp and an internal and external UVB/UVC cut-off filter. The corresponding unirradiated sample sat underneath the

irradiated sample, wrapped in foil to protect it from light, with the irradiated samples placed at a distance of 21.5 cm from the light source.

2-step cellular fixation. 50 mg of disuccinimidyl glutarate (DSG, Thermo Scientific) solvated in DMSO was freshly made and added to PBS about 10 min prior to completion of the cellular irradiation. Upon completion of irradiation, the solution of 2.5 μM Nutlin-3 in PBS was decanted from each 500 cm^2 plate and the cells were washed once with 4 °C PBS; caution was taken to ensure that the plates did not dry out at any point of the procedure. After removing the wash PBS from the plates, 60 mL of 3 mM DSG in PBS at 4 °C was added to each plate and fixation was allowed to proceed for 2 h at 4 °C. During this incubation, the plates sat directly on the metal bench-top in the cold room, covered with foil to prevent further light exposure, and covered with bags of ice. After 2h, the DSG solution was decanted and the plates were washed twice with ambient temperature PBS. The cells were subsequently fixed with 70 mL of 1% formaldehyde (16% formaldehyde single use methanol-free ampule, Thermo Scientific) for 15 minutes at ambient temperature while gently shaking. Formaldehyde crosslinking was quenched by the addition glycine in molar excess, and allowed to shake for 5 min.

The doubly fixed cells were then washed twice with 4 °C PBS, followed by 10 ml of 0.5 mM phenylmethanesulfonylfluoride (PMSF) in 4 °C PBS, made from a 100 mM PMSF in isopropanol stock solution.[13] The cells were then harvested by scraping and isolated by centrifugation. The plates were treated once more with 10 ml of 0.5 mM PMSF, scraped, and combined with the fist pellet. After a second centrifugation, the pelleted cells were frozen in liquid nitrogen, and stored at -80 °C.

Coupling of antibody to magnetic beads. The following procedures were all preformed at 4 °C. Dynabeads goat-anti-mouse IgG magnetic beads (Invitrogen), 50 µL per experiment, were prepared simultaneously for all replicates. The desired amount of Dynabeads was placed in a 15 ml falcon tube and the volume adjusted to 15 ml with sterile filtered 5 mg/ml BSA in PBS. The beads were then mixed by gentle rotation for 5 min, magnetically collected for 5 min, and the supernatant carefully decanted. This wash procedure was then repeated twice more. The beads were then treated with 10 µl of monoclonal DO-7 antibody per 50 µl of Dynabeads in a total volume of 10 ml PBS with 5 mg/ml BSA. The antibody conjugation was allowed to precede overnight at 4 °C while gently rotating.

Chromatin isolation and sonication. The cells were removed from storage at -80 °C and allowed to thaw on ice in 10 ml of Farnham lysis buffer (5 mM PIPES, pH 8.0, 85 mM KCl, 0.5% NP-40, with one complete protease inhibitor tablet per 50 ml (Roche)) and allow to gently rotate for 15 min.[13] To isolate the nuclear pellet, the solution was centrifuged for 5 min at 2000 RPM, and supernatant decanted. The nuclear pellet was then suspended 1.0 ml of RIPA buffer (1x PBS, 1% NP-40, 0.5% sodium deoxycholate, 0.1% SDS, with one complete protease inhibitor tablet per 50 mL) and transferred to a 1.7 ml flat bottom eppendorff tube.[13] To shear the chromatin, the solution was then sonicated with a QSonica sonifier with microtip at 45% power for 30 sec on and 59 sec off for 20 rounds. To prevent heating of the sample, the sample was held within a -20 °C ethanol bath. The sonicated was cleared by centrifugation in a tapered 1.5 ml eppendorff tube at 14,000 rpm for 15 minutes. The supernatant was then transferred to a clean tube, without disturbing the pellet, and the protein concentration determined via

BCA assay as per manufacturer protocol. This will yield enough sample for 3 or 4 replicates per condition, and at least 100 µl of this solution is to be saved for input analysis and sonication control.

Chromatin immunoprecipitation. As the BCA assay incubated, the DO-7 treated Dynabeads were washed three times, as described above, with 5 mg/ml BSA in PBS. At this point, the beads are to be equally divided into 1.5 mL eppendorf tubes respective to the number of samples and replicates in preparation. To each sample, 100 µl of 5 mg/ml BSA in PBS, 1 mg total protein content of chromatin sonicate (as determined by BCA), and RIPA buffer up to 1 ml total volume were added and incubated while rotating at 4 °C for 16-24 h.

To ensure equivalent sonication among all samples, 50 µl of each sample condition chromatin was treated with 150 µl of elution buffer (1% SDS in 0.1 M $NaHCO_3$) and incubated at 65 °C overnight for crosslink reversal.[13] These samples were purified with the Qiagen DNeasy kit, dried, and run on a 1% agarose gel in 1% TBE and ethidium bromide for visualization.

Chromatin washing and elution. Due to overnight rotation, magnetic beads may stick to the eppendorf cap. The samples are briefly centrifuged and washed 5 times with 1 ml of LiCl wash buffer (100 mM Tris, 500 mM LiCl, 1% NP-40, and 1% deoxycholate) with 10 min rotational mixing, and 5 min magnetic isolation.[13] After the final wash, the beads were suspended in TE buffer (10 mM Tris, pH 8.0, 1 mM EDTA) and transferred to O-ring screw cap tubes.[13] The beads were then magnetically isolated once more and suspended in 200 µl IP Elution buffer (1% SDS in 0.1 M $NaHCO_3$) and incubated at 65 °C for 16 h, vortexing intermittently.[13]

Purification of immunoprecipitated DNA. To isolate and purify the immunoprecipitated chromatin, the solution was extracted once with 200 µl of phenol/$CHCl_3$ /isoamyl alcohol (Sigma). The mixture was vortexed thoroughly and centrifuged at 14,000 RPM for 10 min for phase separation. The aqueous phase was then transferred to a clean eppendorf tube. The remaining organic phase was then back-extracted once with 100 µl of elution buffer, as above, and pooled the first aqueous phase. The isolated chromatin was then purified using the Qiagen PCR cleanup kit as per manufacturer protocol, with the final sample eluted twice with 100 µl of buffer EB.

Quantitative PCR reactions. qPCR was conducted on a Bio-Rad CFX 96 real time PCR platform. Individual reactions were carried out at a total reaction volume of 20 µl per well, in a 96 well low-profile PCR plate. Samples were composed of 2x SybreGreen Supermix (Roche), 50 µM primers, 2.0 µL of ChIP DNA isolate, and the respective amount of water. A two-step amplification method was used, followed by melting curve determination. The qPCR procedure used was as follows: 10 min denaturing at 95 °C, followed by 45 cycles of 10 sec for denaturing at 95 °C, and 30 sec for annealing and amplification at 63 °C, reading the plate fluorescent intensity after each cycle. The melting curve was determined over a range of 65 °C to 95 °C with plate reads taken at 0.5 °C intervals.

Quantitation of qPCR data. These data are first analyzed by the comparative Ct method (ΔΔCt), determining the fold change in p53 occupancy of each sample with respect to its non-immmunoprcipitated control.

$$\Delta Ct = Ct\ (ChIP\ sample) - Ct\ (Input\ sample)$$

$$\Delta\Delta Ct = [Ct\ (ChIP\ sample, Dark) - Ct\ (Input\ sample, Dark)] - [Ct\ (ChIP\ sample, Light) - Ct\ (Input\ sample, Light)]$$

Samples: (-Rh Dark) — no photooxidant treatment and uniradiated.

(-Rh Light) — no photooxidant treatment and irradiated.

(+Rh Dark) — treated with $[Rh(phi)_2(bpy)]^{3+}$ and uniradiated.

(+Rh Light) — treated with $[Rh(phi)_2(bpy)]^{3+}$ and iradiated.

Once the ΔΔCT values are determined, the ratio of the target p53 site relative to the untreated sample can be determined by taking $2^{\Delta\Delta Ct}$. The overall change in p53 occupancy induced by DNA CT is determined, where positive values indicate an increase in p53 occupancy at the response element site and negative values indicate decreased p53 occupancy, as described below:

$$2^{[\Delta\Delta Ct\ (+Rh)]} - 2^{[\Delta\Delta Ct\ (-Rh)]} = change\ in\ p53\ occupancy\ under\ oxidative\ DNA\ CT$$

Genetic sequencing of genome wide p53 occupancy by chromatin immunoprecipitation of $[Rh(phi)_2bpy]^{3+}$ treated HCT116N cells. Samples were prepared as described above, but the majority of the isolated chromatin sample was not subject to qPCR. The concentrations of the samples were determined through Qubit fluorescent analysis. The purified samples were subsequently made into Illumina sequencing libraries (TruSeq ChIP Sample Prep Kit, Illumina), and sequenced on the

Illumina Next-Gen sequencing platform using the C23KDACXX 50 base pair single ended flowcell.[14] The determined reads were mapped to the hg19 human genome using the Bowtie program to create genome coverage plots.[15] The data were then imported to and visualized through the UCSC genome browser.[16] The program MACS2 was used for model-based Analysis for ChIP-Seq, which called peaks of statistical significance.[17] Overall, 18489 peaks were called. Of those peaks, the top 20 were chosen to be further investigated by qPCR. Digital resources for the sequencing data are located in Appendix 3.2 and 3.3.

RESULTS

ChIP-qPCR.

The raw data obtained by qPCR were analyzed using the ΔΔCT method over ten experimental replicates. Since the addition of the Rh photooxidant influences p53 binding, the data were first normalized to the respective irradiated controls for both the –Rh and +Rh sample pairs. Once each sample set was normalized to their respective unirradiated control, the change in p53 occupancy due to oxidative DNA CT can be determined through the difference observed between the –Rh sample set and the +Rh sample set. It was found that the results were widely variable among all ten sample sets, including both increased and decreased p53 occupancy at the three investigated response elements. The determined change in p53 occupancy is depicted graphically in Figure 3.2 and corresponding values are listed in Table 3.1. The floating bar depiction of the ChIP-qPCR data in Figure 3.2 depicts the 25th and 75th percentiles of the observed data in the boxed region, while the whiskers represent the 5th and 95th percentiles, and the solid bar

FIGURE 3.2 — Floating bar plot of ChIP-qPCR experimental results. The floating bar depiction of the column of boxed data represents the 25th and 75th percentiles, while the whiskers represent the 5th and 95th percentiles. The solid bar within the box represents the median value.

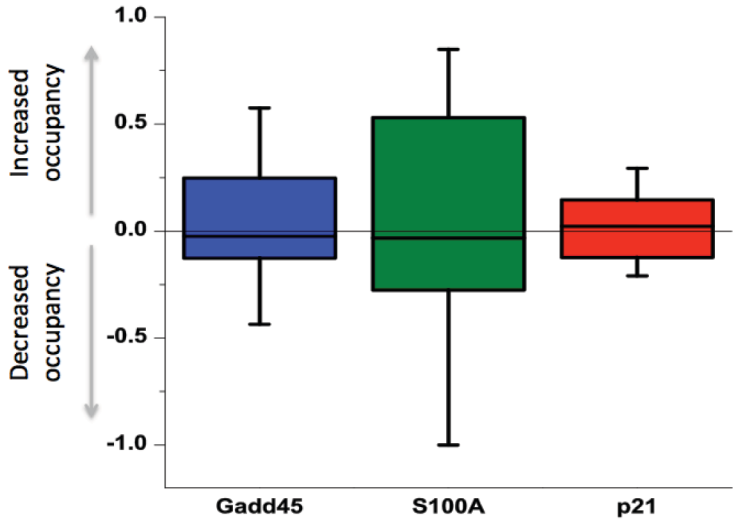

TABLE 3.1 — Change in p53 occupancy for the +Rh–irradiated samples as determined by the ΔΔCT method.

Exp. Date	Gadd45	S100A	p21
20130325	-0.125	-0.651	0.164
20130301	0.326	0.213	0.352
20130204	0.575	0.529	0.294
20121217	-0.041	-0.276	-0.124
20121126	-0.262	-0.269	-0.209
20121106	0.332	0.849	0.007
20121031	-0.009	-0.046	-0.018
20121021	-0.437	-1.001	-0.147
20120911	-0.126	-0.021	0.039
20121204	0.247	0.619	0.146
Avg.	0.048	-0.005	0.050

within each box represents the median value.

In the case of the p21 response element (red in Figure 3.2), we anticipated to observe minimal p53 dissociation based upon results observed in EMSA assays, corresponding to a minimal change in p53 occupancy. As normalized to the -Rh-unirradiated control, we observe p53 dissociation in the +Rh unirradiated sample, and both increased and decreased p53 occupancy within the -Rh irradiated control. When determining the overall fold change in occupancy with respect to oxidative DNA CT, we observe what appears to be a reasonable average of the two controls, with the majority of the samples being within limits of the dark and untreated control. The maximum fold decrease for p21 was determined at -0.209 and a maximum increase at +0.35, giving a total range of change of 0.559.

With respect to the Gadd45 response element (blue in Figure 3.2), we anticipated observing a large trend toward decreased p53 occupancy, since p53 readily dissociates from this response element *in vitro*. Overall, with respect to the unirradiated controls, the change in p53 occupancy based upon oxidative DNA CT was a dramatically varied distribution of both increased and decreased p53 occupancy. However, it appears that the majority of the replicates displayed decreased p53 occupancy. The maximum fold decrease for Gadd45 was determined at -0.437 and a maximum increase at +0.575, giving a total range of change of 1.048.

For the S100A response element (green), we anticipated a large trend toward decreased p53 occupancy, since p53 dissociation was observed *in virto.* Overall, an extraordinarily variable change in occupancy is observed, with both increased and

decreased occupancy. The maximum fold decrease for Gadd45 was determined at -1.001 and a maximum increase at +0.849, giving a total range of change of 1.85.

ChIP-Sequencing.

One set of ChIP samples were run on the Illumina Nex-Gen sequencing platform, comparing the four samples conditions against input, not immunoprecipitated, samples. The determined fragments were correspondingly mapped to the hg19 human genome, allowing us to observe density reads, as well as fold enrichment.[15-17] Links to these data are located in Appendix 3.2. Using a Model-based Analysis for ChIP-Seq, 18489 peaks of statistically significant chromatin enrichment were called. Of those peaks, the top 20 were investigated, p53 response elements determined, and then p53 occupancy investigated by qPCR in our former sets of ChIP isolates. For the genomic locations of interest, the response elements within them are located in Table 3.2. qPCR analysis was conducted upon four ChIP chromatin sets. The results for these enriched sequences also displayed significant variations in p53 occupancy, both increased and decreased. These data and variability determined are depicted in Table 3.3, and the corresponding primer sequences used in this analysis are located in Appendix table 3.1. These results led us to conclude that using ChIP qPCR to determine p53 occupancy *in cellulo* is a difficult task with inherent variability too large to successfully achieve our desired goal of monitoring p53 function in response to oxidative genomic stress.

DISCUSSION

Although the ChIP-qPCR result for Gadd45, S100A, and p21 were highly variable, and showed increased p53 occupancy on the response element sites

when only decreased p53 occupancy was anticipated, one interesting trend did emerge. In the case of S100A and Gadd45, the two response elements from which oxidative dissociation was observed *in vitro*, we observed a wide range of decreased and increased p53 occupancy. For Gadd45, we observed change in p53 occupancy from -0.437 to +0.575; a range of change of 1.048. For S100A, we observed even wider changes in p53 occupancy from -1.001, and the maximum and median values determined over the ten experimental replicates were both negative values, suggesting a slight preference toward p53 dissociation. However, on the sequence that we did not anticipate dissociation from, p21, we observed a much more narrow range than in the change of p53 occupancy. For p21, we observed change in p53 occupancy from -0.209 to +0.35, a range of change of 0.559. For the p21 response element, the determined median value was positive, suggesting p53 does not preferentially dissociate from this sequence. Although a well-defined response of p53 to genomic oxidative stress has yet to be observed *in cellulo*, our results via ChIP-qPCR may suggest that our predications about responsiveness based on response element DNA sequence may be valid. We can correlate the predicted responsiveness of a p53 response element to an increased amount of variability of p53 occupancy *in cellulo* during oxidative genomic stress. As for the response elements we would anticipate to be not responsive, substantially less variability in p53 occupancy will be observed at those response elements under oxidative genomic stress. However, determining whether an increase or a decrease in p53 occupancy will occur remains elusive.

TABLE 3.2 — Significant peaks as determined by ChIP-Seq and evaluated by ChIP-qPCR. p53 response elements located within most significant peaks as determined by ChIP-Seq.analysis. qPCR was used to determined the relative p53 occupancy determined for the +Rh–irradiated samples as calculated by the ΔΔCT methods with green indicating increased occupancy and red indicating decreased occupancy.

Peak Rank	Response Element (5'-3')	Genomic Location	A	B	C	D
1	AGACATGCCTGAACATGCCCAGGCATGTCCCAGCTTGCAG	chr17: 37,203,119-37,203,158	1.90	0.27	0.02	1.33
2	GAACATGCCCAGGCATGTCT	chr2: 70,824,222-70,824,241	0.97	0.09	-0.33	0.70
3	GGGCATGCCCAGACAAGCCC	chr7: 40,757,090-40,757,109	1.34	0.57	-0.47	0.40
4	GGACATGTCTGGGCATGTCC	chr6: 31,305,110-31,305,129	0.81	0.08	-0.19	-0.04
5	AGGCATGCCCGGGCATGTCT	chr1: 181,104,278-181,104,297	-0.08	1.39	-0.41	-1.75
6	GGACATGTTGGGACATGCCA	chr8: 29,628,142-29,628,161	1.34	-0.14	0.25	0.15
7	GAACATGTCC	chr18: 3,305,487-3,305,496	n/a	0.44	-1.88	0.87
8	GGGCATGTTGGGACATGCCT	chr4: 41,146,994-41,147,013	0.15	2.54	-0.22	-1.65
9	AGGCATGTCTGGACATGTCT	chr7: 121,151,349-121,151,368	1.19	0.11	-0.36	-0.02
10	AGACATGTTCAGACATGCCT	chr21: 34,739,689-34,739,708	2.08	0.03	-0.21	1.18
11	GAACATGTCTGGGACATGTTC	chr7: 123,886,643-123,886,663	n/a	0.12	0.29	0.96
12	ATACATGTCCAAACATGCCC	chr16: 20,877,270-20,877,289	n/a	0.51	0.16	1.02
13	AAACATGTCAGGACATGCCT	chr1: 234,754,327-234,754,346	1.49	-0.08	0.23	0.81
15	GGACATGCCTGGGCATGTCC	chr6: 151,178,483-151,178,502	4.14	0.29	1.28	-0.43
17	GGGCATGCCTGGGCATGCCT	chr9: 114,907,243-114,907,262	0.02	2.74	0.07	-0.08
19a	GGGCTTGTCTAAGACATGCCC	chr1: 244,898,865-244,898,885	-0.11	2.36	1.25	0.90
19b	GACTTGCCCCAGACATGCCC	chr1: 244,898,918-244,898,936	0.10	1.17	0.13	0.43
20	AGGCTAGCCCAGGCATGTTC	chr9: 84,636,327-84,636,346	1.90	0.27	0.02	1.33
21b	ACACATGCCTGGACATGCCC	chr4: 84,092,282-84,092,301	2.01	0.04	1.40	0.57

The genomic sequencing of one set of ChIP DNA samples revealed to us a large pool of information about the DNA to which p53 binds. Overall, more than 18,000 genomic locations were found to be enriched by anti-p53 ChIP. Aligning the data to the human genome (hg19), we were able to compare the overall enrichment, over the non-immunoprecipitated input sample, of the four sample conditions in comparison to one another. It was evident in these profiles that increases in genomic material around certain response elements also occurs in the +Rh-irradiated samples, as compared to the respective controls. This finding confirms that the increased occupancy observed in the ChIP-qPCR experiments is a real phenomenon.

From the best peaks determined through the MACS2 program, most were found to contain p53 response element DNA patterns within those genomic locations, and primers were designed to conduct qPCR on these new sites of interest. Of the samples determined through sequencing and re-evaluated in the ChIP samples, we again observed large ranges of variability among the four sample sets tested, and continued testing was felt to be futile.

These results highlight the intricacies of transcription factor p53 gene regulation and the level of complexity and variation that can occur *in cellulo*. The study of p53 *in cellulo* has been complex, extensive, and left us with more questions than answers. There is much still to be learned about the role of p53 in response to genomic oxidative stress and how it interacts with DNA. Before further *in cellulo* experiments are undertaken, a cleaner approach to inducing DNA CT must be devised. These studies merely confirm the eloquently stated

words by Karen H. Vousden and Carol Prives: “If genius is the ability to reduce the complicated to the simple, then the study of p53 makes fools of us all.”[18]

REFERENCES

1. Riley, T., Sontag, E., Chen, P., and Levine, A. (2008) Transcriptional control of human p53-regulated genes. *Nat. Rev. Mol. Cell Biol. 9*, 402-412.

2. Wei, C. L., Wu, Q., Vega, V.B., Chiu, K. P., Ng, P., Zhang, T., Shahab, A., Yong, H. C., Fu, Y., Weng, Z., Liu, J., Zhao, X. D., Chew, J. L., Lee, Y. L., Kuznetsov, V. A., Sung, W. K., Miller, L. D., Lim, B., Liu, E. T., Yu, Q., Ng, H. H., and Ruan, Y. (2006) A Global Map of p53 Transcription-Factor Binding Sites in the Human Genome. *Cell 124*, 207-219.

3. Hattori, H., Janky, R., Nietfeld, W., Aerts, S., Madan Babu, M., and Venkitaraman, A. R. (2014) p53 shapes genome-wide and cell type-specific changes in microRNA expression during the human DNA damage response. *Cell Cycle 13*, 2572-2586.

4. Schaefer, K. N., and Barton, J. K. (2014) DNA-mediated oxidation of p53. *Biochemistry 53*, 3467-3475.

5. Geil, W. M. (2012) Regulation of wild-type and mutant p53 through DNA-mediated charge transport. Dissertation Ph.D., California Institute of Technology.

6. Fischer, M., Steiner, L., and Engeland, K. (2014) The transcription factor p53: Not a repressor, solely an activator. *Cell Cycle 13*, 3037-3058.

7. Gupta, S., Radha, V., Furukawa, Y., and Swarup, G. (2001) Direct Transcriptional Activation of Human Caspase-1 by Tumor Suppressor p53. *J. Biol. Chem. 276*, 10585-10588.

8. Wicki, R., Franz, C., Scholl, F. A., Heizmann, C. W., and Schäfer, B. W. (1997) Repression of the candidate tumor suppressor gene S100A2 in breast cancer is mediated by site-specific hypermethylation. *Cell Calcium 22*, 243-254.

9. Cao, L. Y., Yin, Y., Li, H., Jiang, Y., and Zhang, H. F. (2009) Expression and clinical significance of S100A2 and p63 in esophageal carcinoma. *World J. Gastroenterol. 15*, 4183-4188.

10. Mirza, A., Wu, Q., Wang, L., McClanahan, T., Bishop, W. R., Gheyas, F., Ding, W., Hutchins, B., Hockenberry, T., Kirschmeier, P., Greene, J. R., and Liu, S. (2002) Global transcriptional program of p53 target genes during the process of apoptosis and cell cycle progressions. *Oncogene*. *22*, 3645-3654.

11. Liu, S., Mirza, A., and Wang, L. (2004) Generation of p53 target database via integration of microarray and global p53 DNA-binding site analysis. *Methods Mol. Biol. 281*, 33-54.

12. Hall, D., Holmlin, R., and Barton, J. (1996) Oxidative DNA damage through long-range electron transfer. *Nature 382*, 731-735.

13. Wells, J., and Farnham, P. J. (2002) Characterizing transcription factor binding sites using formaldehyde crosslinking and immunoprecipitation. *Methods 26*, 48-56.

14. Sequencing Methods Review, a review of publications featuring Illumina Technology. http://www.illumina.com/content/dam/illumina-marketing/documents/products/research_reviews/sequencing-methods-review.pdf

15. Langmead, B., Trapnell, C., Pop, M., and Salzberg, S. L. (2009) Ultrafast and memory-efficient alignment of short DNA sequences to the human genome. *Genome Biol 10*, R25.

16. Kent, W. J., Sugnet, C. W., Furey, T. S., Roskin, K. M., Pringle, T. H., Zahler, A. M., and Haussler, D. (2002) The human genome browser at UCSC. *Genome Res. 12*, 996-1006.

17. Zhang, Y., Liu, T., Meyer, C., Eeckhoute, J., Johnson, D., Bernstein, B., Nusbaum, C., Myers, R., Brown, M., Li, W., and Liu, X. (2008) Model-based Analysis of ChIP-Seq (MACS). *Genome Biol. 9*, R137.

18. Vousden, K., and Prives, C. (2009) Blinded by the Light: The Growing Complexity of p53. *Cell 137*, 413-431.

Appendix 3.1 — Example gel shift of upregulation of p53 via Nutlin-3 treatments (top). Example of sonication gel of chromatin prepared for ChIP (bottom).

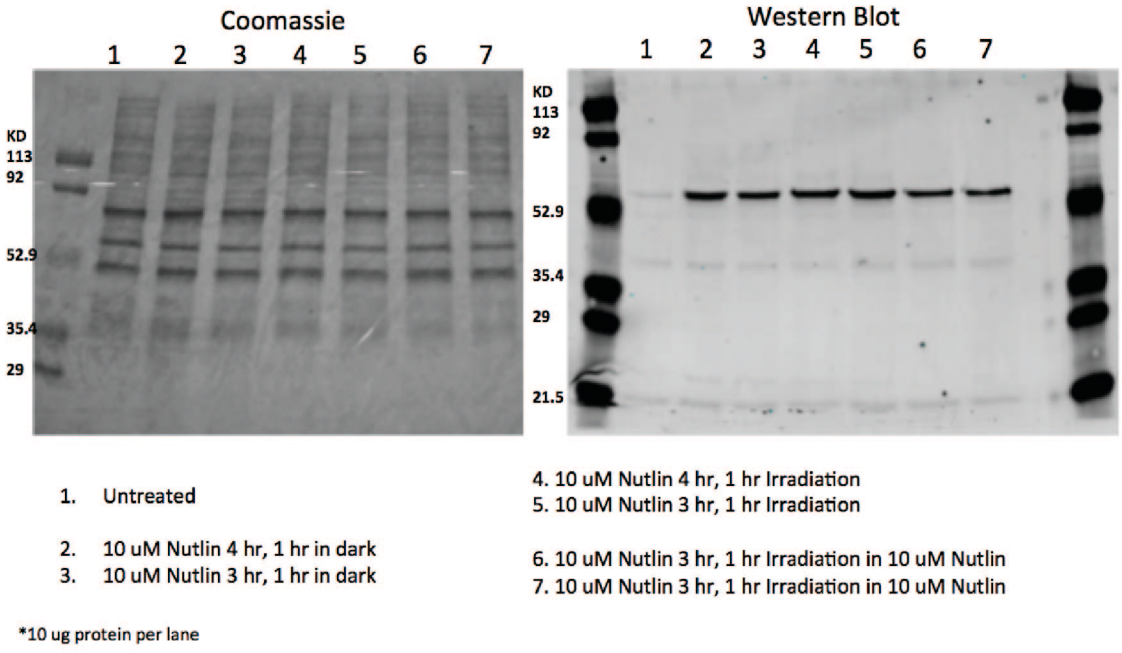

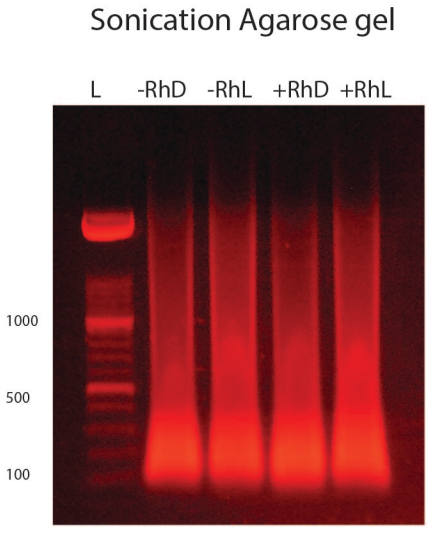

Appendix 3.2

The following libraries are on the flowcell C23KDACXX, which is a 50 base pair single ended flowcell:

Lane : (Library Id) Library Name (Cluster Estimate)

Lane #4 : (13682) index # 10 Rh Dark HCT116N p53 (None)

https://jumpgate.caltech.edu/library/13682

Lane #4 : (13683) Index #11 Rh Light HCT116N p53 (None)

https://jumpgate.caltech.edu/library/13683

Lane #4 : (13679) Index # 4 Input of HCT116N ChIP (None)

https://jumpgate.caltech.edu/library/13679

Lane #4 : (13680) Index #5 Untreated Dark HCT116N p53 (None)

https://jumpgate.caltech.edu/library/13680

Lane #4 : (13681) Index #7 Untreated Light HCT116N p53 (None)

https://jumpgate.caltech.edu/library/13681

Appendix 3.3

Genome browser data:

http://genome.ucsc.edu/cgi-bin/hgTracks?db=hg19&hgct_customText=track%20type=bigWig%20name=%22Input%22%20visibility=full%20color=64,64,64%20bigDataUrl=http://cheget.caltech.edu/~igor/tempHtml/KatieSchaefer/13679_input.wig.bigWig

http://genome.ucsc.edu/cgi-bin/hgTracks?db=hg19&hgct_customText=track%20type=bigWig%20name=%22Untreated_dark%22%20visibility=full%20color=128,0,128%20bigDataUrl=http://cheget.caltech.edu/~igor/tempHtml/KatieSchaefer/13680_untreated_dark.wig.bigWig

http://genome.ucsc.edu/cgi-bin/hgTracks?db=hg19&hgct_customText=track%20type=bigWig%20name=%22Untreated_light%22%20visibility=full%20color=128,0,0%20bigDataUrl=http://cheget.caltech.edu/~igor/tempHtml/KatieSchaefer/13681_untreated_light.wig.bigWig

http://genome.ucsc.edu/cgi-bin/hgTracks?db=hg19&hgct_customText=track%20type=bigWig%20name=%22Rh_dark%22%20visibility=full%20color=0,128,0%20bigDataUrl=http://cheget.caltech.edu/~igor/tempHtml/KatieSchaefer/13682_rh_dark.wig.bigWig

http://genome.ucsc.edu/cgi-bin/hgTracks?db=hg19&hgct_customText=track%20type=bigWig%20name=%22Rh_light%22%20visibility=full%20color=0,0,128%20bigDataUrl=http://cheget.caltech.edu/~igor/tempHtml/KatieSchaefer/13683_rh_light.wig.bigWig

Fold enrichment tracks:

http://genome.ucsc.edu/cgi-bin/hgTracks?db=hg19&hgct_customText=track%20type=bigWig%20name=%22Untreated_dark_FE%22%20visibility=full%20color=128,0,128%20bigDataUrl=http://cheget.caltech.edu/~igor/tempHtml/KatieSchaefer/untreated_dark_gb_FE.bigWig

http://genome.ucsc.edu/cgi-bin/hgTracks?db=hg19&hgct_customText=track%20type=bigWig%20name=%22Untreated_light_FE%22%20visibility=full%20color=128,0,0%20bigDataUrl=http://cheget.caltech.edu/~igor/tempHtml/KatieSchaefer/untreated_light_gb_FE.bigWig

http://genome.ucsc.edu/cgi-bin/hgTracks?db=hg19&hgct_customText=track%20type=bigWig%20name=%22Rh_dark_FE%22%20visibility=full%20color=0,128,0%20bigDataUrl=http://cheget.caltech.edu/~igor/tempHtml/KatieSchaefer/rh_dark_gb_FE.bigWig

http://genome.ucsc.edu/cgi-bin/hgTracks?db=hg19&hgct_customText=track%20type=bigWig%20name=%22Rh_light_FE%22%20visibility=full%20color=0,0,128%20bigDataUrl=http://cheget.caltech.edu/~igor/tempHtml/KatieSchaefer/rh_light_gb_FE.bigWig

Appendix 3.4 — qPCR primers for peaks determined through ChIP-Seq.

Peak	Forward Primer (5´-3´)	Reverse Primer (5´-3´)
1	ATGCCCAGGCATGTCCCAGCTT	ACGCACTGGGCTTCTACTGCTGTGT
2	ACGTGCGTGGTAGCAGGTGGTCTGCTT	ACGTGCGTGGTAGCAGGTGGTCTGCTT
3	TCCTCCCGTGCACAAGGCGTGAACT	GCAAATGAGGGAACCTGCCCAGGGCTT
4	TCCTGTCTCCATTGGCTGGAACTGGACC	CCTAGTCTGCCTGGATCTGCCTGGACA
5	TGTCCCTGGGTGTCTGCATCTGCGT	ACTCGGGCGTTCTCTCCATGCCTCAGA
6	TGGTAATGCCTTCTCTGGAACTTTGCCTGC	TGCTGGCATGTCCCAACATGTCCCAA
7	GCCTATGTGTGTAGGAGGCTAGACCATCTAGGTTT	TGCACGGGCTGCATTCATGCCTCA
8	CCAGACGTTCAAGACCAGCCTGGGCAA	ATAGCTGGGCCCACAGGCATGTCCCAA
9	TCCCTGTGTCTAGGGTTGGACTGCACA	TCCAGCCTGCCAACAACTCTCCCACT
10	TCCGCTCTGATTGTGCCCTGACATGC	CCCGCATGCAGCTTCTGTTCCTGTGT
11	AGACGAGACTAAGGGTTCATATAATGGGTCAGGGT	ACCAGTCAGCAGCACCACAAAGGTACGCA
12	CCCTTCTCCACCCGCAAAGAGAGCA	CCCTTGTACCATGGTCTTCCAAGAATTAACCC
13	AGCCTGGAATGCTGAAACCCTCTTAGACTGAA	AGTACGGAATGTGGAATTCTGAGCCTAAACCGT
15	TCCATTGGCTGGAGCCAGACCTCACA	TCCTTGTACCTTAGTCAGAATATTCGTGCTGGACA
17	ATGCCTGGGCATGCCTATGGTCCCAGT	CCTCCTGCCTCAGCCTCTTGAGCAACT
19A	AATCCGGTCAGGCAGGCAGTTAGGGTG	TCCATTGCGGGCATGTCTGGGCAAGT
19B	GCCCACAGCTGCACAGACAAGAAAGCC	ATTGCGGGCATGTCTGGGCAAGTCACC
20	TGTTTGTCTGGAGCTTTGCCTGGGACAC	CATGGACCCTTGCAACCTGCTTAGCCA
21B	GCTGCATGCGCCCTTTGGTGGTTGA	GGAGACTTCTTGACTTGTGGGCAACAACTTCCT